

PAPER • OPEN ACCESS

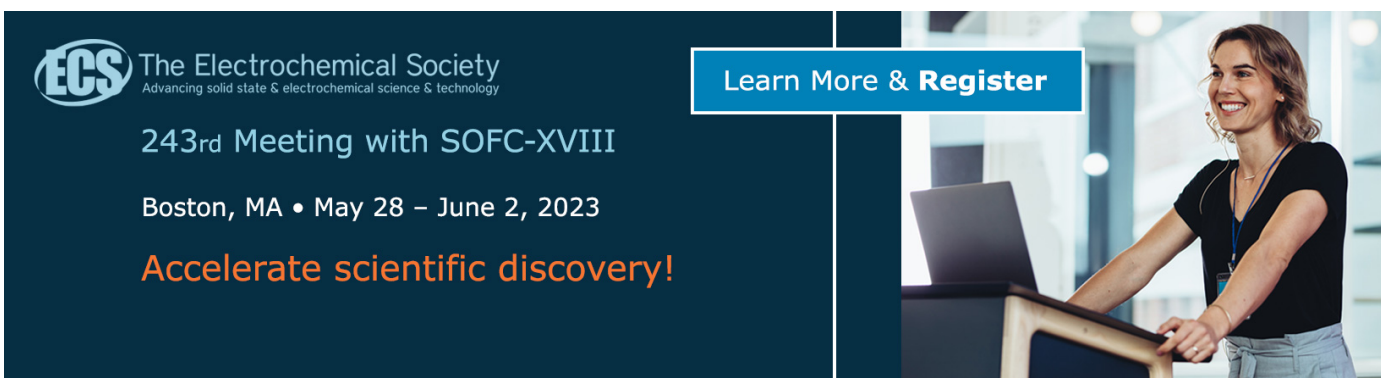
A Study on Accounting for Drift Velocities on Liquid Jets Injected in Cross Flow

To cite this article: Nasrin Sahranavardfard *et al* 2022 *J. Phys.: Conf. Ser.* **2385** 012136

View the [article online](#) for updates and enhancements.

You may also like

- [Controlling Inkjet Fluid Kinematics to Achieve SOFC Cathode Micropatterns](#)
Theresa. Y. Hill, Thomas L. Reitz, Michael A. Rottmayer et al.
- [A hybrid electrohydrodynamic drop-on-demand printing system using a piezoelectric MEMS nozzle](#)
Young-Jae Kim, Sang-Myun Lee, Sangjin Kim et al.
- [The transport dynamics of tens of micrometer-sized water droplets in RF atmospheric pressure glow discharges](#)
Gaurav Nayak, Mackenzie Meyer, Gaku Oinuma et al.



The advertisement features a dark blue background on the left with white and orange text, and a photograph of a woman at a podium on the right. The woman is smiling and looking towards the camera. The background of the photo is a bright, modern interior with large windows.

ECS The Electrochemical Society
Advancing solid state & electrochemical science & technology

243rd Meeting with SOFC-XVIII

Boston, MA • May 28 – June 2, 2023

Accelerate scientific discovery!

Learn More & Register

A Study on Accounting for Drift Velocities on Liquid Jets Injected in Cross Flow

Nasrin Sahranavardfard^{1,3}, Adrian Pandal², Faniry Nadia Zazaravaka Rahantamialisoa¹, Michele Battistoni¹

¹ Department of Engineering, University of Perugia, Perugia, Italy

² Department of Energy, Universidad de Oviedo, Gijon, Spain

³ nasrin.sahranavardfard@studenti.unipg.it

Abstract. The efficiency and combustion performance of propulsion systems, like internal combustion (IC) engines and gas turbines, is known to be related to the performance of the fuel and air mixing process. Operating conditions and fuels are rapidly changing, therefore new CFD models which accurately accounts for all physical aspects, still maintaining a simple framework, are extremely important. In this work we consider the drift velocity contribution, which often is overlooked or neglected, defined as the velocity of the dispersed phase relative to the mixture volumetric mean velocity in a single fluid formulation, a key variable in two-phase mixture model. Water test cases are here considered for the study. The present work investigates the structure and the droplet velocity field of a plain liquid jet injected into a high-pressure air crossflow. Because of the large scale separation between the small features of the interface and the overall jet we use the diffuse-interface treatment in a single-fluid Eulerian framework. A Σ -Y family model is implemented in the OpenFOAM framework which includes liquid diffusion due to drift-flux velocities and a new formulation of the spray atomization. The main objective is to explore the droplet velocity distribution and the jet structure with and without considering the drift flux correction and compare the related results with the experimental data.

1. Background and objective

Jets injected perpendicularly into a cross-stream can be found in a range of technological systems [1, 2], the jet in crossflow (JICF) or transverse jet is utilized in dilution or primary air jet injection in gas turbine combustors, to accomplish mixture formation and NO_x control as well as turbine hot section cooling; in film cooling of turbine blades; in primary fuel injection in high speed airbreathing engines; and in thrust vector control for missiles and other high speed vehicles [3].

As air travel becomes more popular, polluting emissions like NO_x, soot, and carbon monoxide might cause negative environmental effects. Thus, manufacturers modify their engine concepts in order to reduce their environmental impact. Therefore, advanced technologies have been developed. In order to achieve fine and uniform fuel droplet distribution, manufacturers of combustion chambers developed lean-burning combustion regimes to minimize pollutant formation [4], numerous investigations of the atomization process in constant air flow have been published in the literature. It was demonstrated how different parameters, such as the moment flux ratio or the Weber number, affect the liquid behavior [5, 6, 7]. The development of models for the important phenomena have focused on important dimensionless quantities, such as the Weber number. In this case based on the crossflow properties it is appealing to include these dimensionless groups in the description of behaviors of interest such as penetration, breakup, and atomization of the liquid jet [8].

The basic concept of the drift-flux model is to consider the mixture as a whole, rather than two phases separately. It is clear that the drift-flux model formulation will be simpler than the two-fluid model, so it requires some constitutive assumptions causing some of the important characteristics of two-phase flow to be lost. However, it is exactly this simplicity of the drift-flux model that makes it very useful in many engineering applications. In the drift-flux model formulation we have only four field equations and, thus, one energy and one momentum equation have been eliminated from the original six field



equations. Then, the relative motion and energy difference should be expressed by additional constitutive relations in the mixture balance equations [9]. Ishii [10] has developed a general formulation of the mixture and Ishii [11] has discussed various special cases that are important in practical applications. The drift velocity contribution to two-phase mixture models is often overlooked or ignored in CFD simulations, or closed with inappropriate models. By definition [9] it is the velocity of the dispersed phase relative to the mixture volumetric mean velocity.

For this study, water test cases are considered. In the present study, we analyze droplet distribution caused by a liquid jet injected in to a pressurized air crossflow. In a single-fluid Eulerian framework [12], the diffuse-interface treatment is used due to the large scale separation between the small features of the interface and the overall jet. A Σ -Y family model is implemented in OpenFOAM that includes drift-flux velocity-related liquid diffusion and a new formulation of spray atomization [12]. The purpose of the study is to examine droplet velocity distributions and jet structures with and without drift-flux corrections and compare the results with experimental results.

2. Case setup and numerical model

The reference study we select used an optically accessible, high-pressure apparatus. Schematic of the case geometry is represented in Figure 1 with the dimensions. The injection nozzle is a flat-ended stainless-steel tube with a 6.35 mm outer diameter and a 1 mm injection diameter at the center of the end walls. Before injection, the flow was smoothed with a taper. As shown in Figure 1, experiments were conducted in a chamber measuring 25.4 mm \times 25.4 mm (1" \times 1") with distilled water injected from a nozzle flush with the bottom wall. In order to provide optical accessibility, the test section had three sides made of borofloat glass and a bottom wall made of aluminum. More details of the model hardware can be found in [13, 18]. Also, the properties of flow and operating conditions are shown in Table 1.

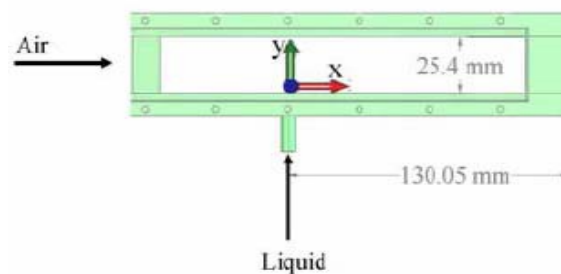


Figure 1. Test section in experimental model [13].

Table 1. Jet in cross-flow operating condition [13, 18], j refers to liquid jet (water) and c refers to cross flow (air).

Parameter	Value
Cross-flow pressure (p_c)	3.00E+05 Pa
Temperature (T)	293.15 K
Water jet density (ρ_j)	1000 kg/m ³
Air cross-flow density (ρ_c)	3.567 kg/m ³
Density ratio (ρ_j/ρ_c)	280.3
Surface tension (σ)	0.07 N/m
Water viscosity (μ_j)	0.001 Pa·s
Injection diameter (d_j)	0.001 m
Momentum flux ratio ($q = \frac{\rho_j U_j^2}{\rho_c U_c^2}$)	20
Weber number ($We_c = \frac{\rho_c U_c^2 d_j}{\sigma}$)	300
Cross flow velocity (U_c)	76.7 m/s
Jet exit velocity (U_j)	20.5 m/s
Jet Reynolds number ($Re_j = \frac{\rho_j U_j d_j}{\mu_j}$)	20461
Cross flow Mach number	0.22

The computational mesh results from a grid convergence study and consists of around 500 k hexahedral cells, with the structure shown in Figure 2. Concerning the boundary conditions, the domain has two inlets and an outlet, while no-slip conditions were selected for the walls. A non-reflective boundary condition is used for the outlet and a time varying velocity condition is used for the inlets where values are initially ramped from zero to the prescribed stabilized values to facilitate the simulation start-up. The air and water inlet velocities are obtained from mass flow rates and momentum flux measurements, applying a constant radial profile of normal velocity and density. In previous works, present configuration has shown remarkable performance [12,21].

Regarding turbulence modelling, present work is focused on the performance of the drift-flux model and thus a fast and not computationally demanding unsteady RANS approach is used to investigate spray development, adopting a high-density ratio $k - \varepsilon$ turbulence model [19].

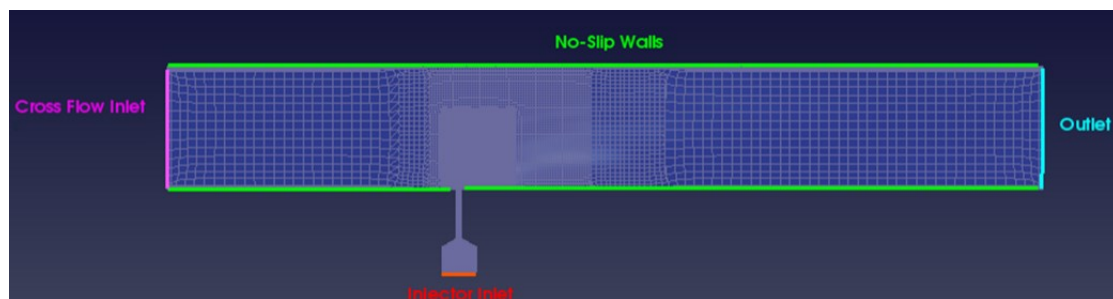


Figure 2. Computational grid and boundary types for CFD model simulations.

3. Drift-flux model description

The proposed atomization model formulation relies on the rigorous conservation equations derived from the theory of two-phase flow mixtures [9]. Two-phase single-fluid theory is also known as drift-flux theory [14], and it is often used to analyze mixtures of closely coupled dynamics, such as diesel sprays. For a turbulent, compressible, two-phase mixture, by introducing the simplifications mentioned in [12], and expressing the macroscopic phase diffusion terms through the drift velocities, the final form of the drift-flux model can be obtained. The balance equations in the final form read as follows:

$$\frac{\partial \rho_m}{\partial t} + \nabla \cdot (\rho_m \mathbf{v}_m) = 0 \quad (1)$$

$$\begin{aligned} & \frac{\partial \bar{\rho}_2 \alpha_2}{\partial t} + \nabla \cdot (\bar{\rho}_2 \alpha_2 \mathbf{v}_m) \\ &= -\nabla \cdot \left(\alpha_2 \frac{\bar{\rho}_1 \bar{\rho}_2}{\rho_m} (1 - \alpha_2) \mathbf{v}_{21,0} \right) + \nabla \cdot \left(\frac{\bar{\rho}_1 \bar{\rho}_2}{\rho_m} (1 - \alpha_2) D_{2m} \nabla \alpha_2 \right) \\ & - \Gamma_{evap} \end{aligned} \quad (2)$$

$$\begin{aligned} & \frac{\partial \rho_m \mathbf{v}_m}{\partial t} + \nabla \cdot (\rho_m \mathbf{v}_m \mathbf{v}_m) \\ &= -\nabla p + \nabla \cdot (\boldsymbol{\tau} + \boldsymbol{\tau}^T) - \nabla \cdot \left(\alpha_2 \frac{\bar{\rho}_1 \bar{\rho}_2}{\rho_m} (1 - \alpha_2) \mathbf{v}_{21,0} \mathbf{v}_{21,0} \right) + \rho_m \mathbf{g}_m \end{aligned} \quad (3)$$

$$\begin{aligned} & \frac{\partial \rho_m h_m}{\partial t} + \nabla \cdot (\rho_m h_m \mathbf{v}_m) \\ &= \nabla \cdot (\mathbf{q} + \mathbf{q}^T) - \nabla \cdot \left(\alpha_2 \frac{\bar{\rho}_1 \bar{\rho}_2}{\rho_m} (\hat{h}_2 - \hat{h}_1) (1 - \alpha_2) \mathbf{v}_{21,0} \right) \\ & + \alpha_2 \frac{\bar{\rho}_1 - \bar{\rho}_2}{\rho_m} (1 - \alpha_2) \mathbf{v}_{21,0} + \frac{Dp}{Dt} + \phi_m^\mu \end{aligned} \quad (4)$$

$$\frac{\partial \tilde{\Sigma}}{\partial t} + \nabla \cdot (\tilde{\Sigma} \mathbf{v}_m) = \nabla \cdot (D_\Sigma \nabla \tilde{\Sigma}) + C_\Sigma \tilde{\Sigma} \left(1 - \frac{\tilde{\Sigma}}{\tilde{\Sigma}_{eq}} \right) + S_{\Sigma_{evap}} + S_{\Sigma_{init}} - \nabla \cdot \left(\tilde{\Sigma} \frac{\bar{\rho}_1}{\rho_m} \mathbf{v}_{2j} \right) \quad (5)$$

where $\rho_m = \alpha_1 \bar{\rho}_1 + \alpha_2 \bar{\rho}_2$ is the mixture density, $\mathbf{v}_m = (\alpha_1 \bar{\rho}_1 \hat{\mathbf{v}}_1 + \alpha_2 \bar{\rho}_2 \hat{\mathbf{v}}_2) / \rho_m$ is the mixture center of mass velocity, and $h_m = (\alpha_1 \bar{\rho}_1 \hat{h}_1 + \alpha_2 \bar{\rho}_2 \hat{h}_2) / \rho_m$ is the mixture enthalpy. The first two equations represent the conservation of total mass and of the secondary phase mass, where α_2 is the liquid (secondary phase) volume fraction, $\bar{\rho}_2$ is the liquid phase averaged density, D_{2m} is the diffusion coefficient of phase-2 in the mixture, and Γ_{evap} is the phase change source term set to 0 in the current work. The third equation is the mixture momentum equation, where $\boldsymbol{\tau}$ is the average viscous stress, $\boldsymbol{\tau}^T$ is the turbulent stress, \mathbf{g}_m expresses body accelerations on the mixture, and p is the pressure. Similarly, the fourth equation is the energy balance for the mixture, expressed in terms of mixture enthalpy h_m . In this equation \mathbf{q} is the average conduction heat flux, and \mathbf{q}^T is the turbulent heat flux. The remaining term collectively express the work done by viscous dissipations, ϕ_m^μ . Finally, the last equation (Eq. 5) expresses the interfacial surface area transport [12]. Also, a turbulence model has to be included, and in this case a U-RANS approach has been used, with a modified form of the k- ϵ model [19] which incorporates the influence of variable density. This set of equations forms the full drift-flux model.

It should be noted that $\bar{\rho}_2 \alpha_2 = \rho_m \tilde{Y}_2$, where \tilde{Y}_2 is the liquid mass fraction. In view of this, the secondary phase transport equation (Eq. 2) can also be seen equivalently as the transport equation for the liquid mass fraction.

To obtain the equations as expressed in 1-4, the drift velocity \mathbf{v}_{2j} is formulated according to the following expression [9, 12].

$$\mathbf{v}_{2j} = (1 - \alpha_2)\mathbf{v}_{21} = (1 - \alpha_2)\left(\mathbf{v}_{21,0} - D_{2m}\frac{\nabla\alpha_2}{\alpha_2}\right) \quad (6)$$

where the relative velocity between phases \mathbf{v}_{21} is decomposed in two parts, a terminal velocity part $\mathbf{v}_{21,0}$ and a diffusive part. The solution for the terminal velocity is obtained from the balance with the drag force as follows

$$|\mathbf{v}_{21,0}|\mathbf{v}_{21,0} = \frac{V_D}{A_D} \frac{2}{C_{d,\alpha_2}} \frac{\bar{\rho}_2 - \rho_m}{\bar{\rho}_1} [\mathbf{g}_m - (\mathbf{v}_m \cdot \nabla)\mathbf{v}_m - \frac{\partial\mathbf{v}_m}{\partial t}] \quad (7)$$

As a result, the terminal velocity is a function of the drag coefficient C_{d,α_2} , the volume V_D and the frontal area A_D of the dispersed phase. Considering the dispersed phase in form of droplets, once the atomization has occurred, the geometrical ratio can be evaluated through the droplet Sauter mean diameter.

$$\frac{V_D}{A_D} = \frac{2d_{32}}{3} \quad (8)$$

Regarding the drag coefficient C_{d,α_2} , the model by Rusche and Issa [12, 20] is used which considers the impact of the phase fraction on the drag, as droplets are not isolated. The traditional Schiller-Naumann correlation for a single spherical body C_d is used, and then corrected as a function of α_2 :

$$C_{d,\alpha_2} = C_d \cdot [\exp(K_1\alpha_2) + K_2\alpha_2^{K_3}] \quad (9)$$

Finally, taking advantage of the interfacial surface area density (Σ), together with the mass averaged liquid fraction (\tilde{Y}_2), droplet sizing can be derived, i.e., the local SMD (d_{32}):

$$d_{32} = \frac{6\rho_m\tilde{Y}_2}{\bar{\rho}_2\Sigma} \quad (10)$$

which creates the active coupling between the Σ transport equation (Eq. 5) and the \tilde{Y}_2 transport equation (Eq. 2). Thus atomization quality affects liquid dispersion, which is the novelty of this model. More details can be found in [12].

It is noted that if the drift velocity \mathbf{v}_{2j} is set equal to zero, the model consistently reverts back to the classical Σ -Y model where Σ is just a passive scalar.

The numerical solution is obtained using the Gamma NVD scheme for convection terms discretization and the first order Euler scheme for time derivative terms. The simulation is a fully unsteady-RANS. The flow is evolved over time until the water jet exits the domain at the outlet, then collection of statistics of each relevant variable begins, to obtain average fields for post processing analysis of the steady situation.

4. Results and discussions

First, an analysis of jet morphology is conducted, to provide an overview of the drift-flux and drift-flux with increased atomization models impact. After that, local flow is compared to experiments in terms of jet shape. Finally, mass fraction, droplet sizing, and drift velocity contours are examined in the same conditions, using three cases the original without accounting for drift, and the drift-flux and drift-flux with increased atomization models.

Firstly, jet shape predictions are depicted for the baseline model (no-drift), drift-flux model, and drift-flux model with increased atomization against the experimental measurements [13] in Figure 3 and Figure 4 in which the time-averaged liquid mass fraction contours are shown. Results are reported for the same 3 bar injection pressure condition (given in Table 1) and the outer edge of the jet is shown in Figure 3. The lower match for the base model is clearly visible, while the positive impact of the drift-flux and drift-flux with increased atomization models can be observed. In the examined test case, the original model under-predicts the measurements with the relative error near to 23 percent in jet height at $x=0.010$ m, while the drift-flux one improves the prediction accuracy showing a clear trend with decreased relative error of around 20 percent. This is in line with the expected impact of the drift, which is meant to improve the liquid-gas interfacial exchange models. In particular, a proper prediction of the interfacial area, and thus of the droplet sizes, which is achieved with the increased atomization setup with the relative error of 18 percent, is crucial to obtain better match of the jet dispersion with measurements. With the drift model having a positive impact, discrepancies still remain clearly visible with respect to the data, and this is currently being further investigated. Turbulence models plays a crucial role in this problem, with large density variations and two phases, and possibly non-linear models could offer better performance.

Model assessment begins with the visual comparison of the predicted droplet d_{32} , in Figure 5. A variety of factors affect droplet size and how easily a stream of liquid atomizes after emerging from an orifice. Among these factors are fluid properties such as surface tension, viscosity, and density (see for example, Elkotb et al. [15], Rizkalla and Lefebvre [16], Lefebvre [17]). The no-drift case calculates the diameters as a passive and uses a calibration for Eq. 5 model constants which is taken from our previous work on diesel sprays [12]. The result indicates that the jet does not breakup realistically, being the core liquid jet still intact at the exit of the observation window ($25.4 \text{ mm} \times 25.4 \text{ mm}$), in contrast with experimental evidence [13, 18]. The drift-flux case (middle image in Figure 5), with the same Σ model constants, but including the drift velocity and therefore the coupling, predicts a marginal better atomization level, but still diameters appear large compared to the range of expected values, below $100 \mu\text{m}$. The jet penetration improves, as visible in Figure 3. Better performance is obtained with a more adequate calibration of model constants (coefficients included in C_{Σ} and $\tilde{\Sigma}_{eq}$ terms), as shown by the drift-flux model with increased atomization. In this case, droplet diameters are aligned with expected values, and the jet core is fully broken up after about 10 mm, in accordance with [13, 18].

We also examined the drift velocity contours reported in Figure 6 under the same condition for the two drift-flux cases, i.e. the drift-flux model and the drift-flux model with increased atomization. The drift velocity sensibly modifies the liquid dispersion and therefore its distribution. The drag, accounted for in the Σ equation, is very much responsible for different liquid trajectories, depending on the size. Simulation with the improved atomization setup generates larger drift velocities, therefore more slip between phases, and this is mainly located at the out edge of the jet and in the low speed wake (bottom-right region). The drift magnitude is in the order of 15-30 m/s which makes an impact in a crossflow problem with air traveling at 76 m/s.

The overall jet behavior is not fully retrieved, even with the drift-flux model proposed here, but the effect is sensible, and the model adds more physics to the classical Σ -Y model. More in-dept validation studies are needed, including local velocities and droplet size data, but the current model development is a step forward towards a more predictive single-fluid atomization model.

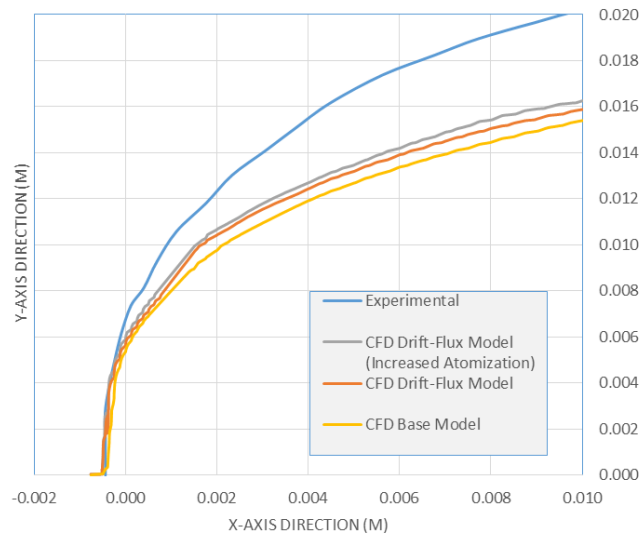


Figure 3. Jet morphology, computed and measured jet tip penetration. Curves represent the jet outer boundary.

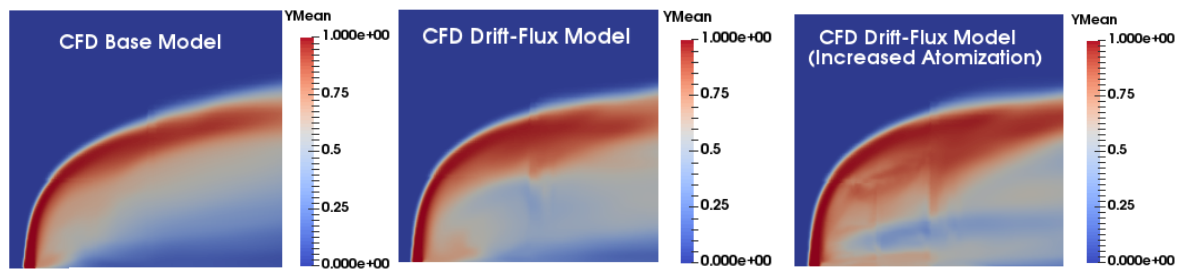


Figure 4. Time-averaged liquid mass fraction contours. CFD uncoupled base model (left), CFD Drift-Flux model (middle), and CFD Drift-Flux model with increased atomization (right).

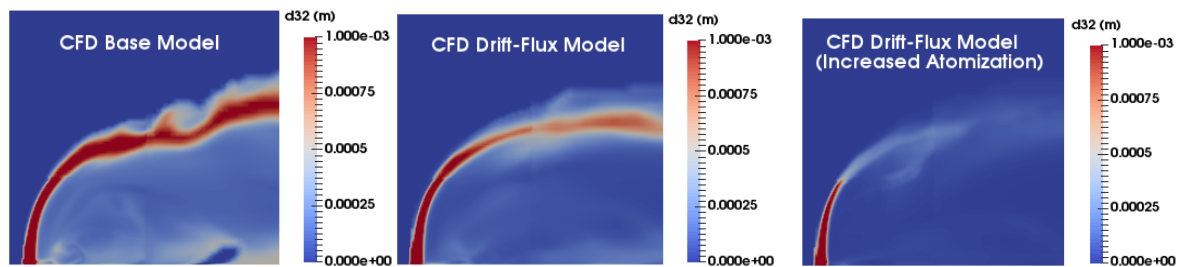


Figure 5. Droplet sizing contours, instantaneous snapshots. CFD uncoupled base model (left), CFD Drift-Flux model (middle), and CFD Drift-Flux model with increased atomization (right).

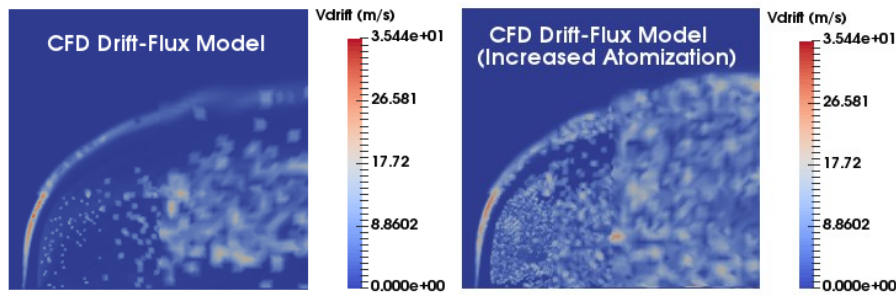


Figure 6. Drift velocity contours, instantaneous snapshots. CFD Drift-Flux model (left) and CFD Drift-Flux model with increased atomization (right).

5. Conclusions

The ultimate goal of this work was exploring the droplet velocity distribution and the jet structure with and without considering the drift flux velocity correction by investigating the structure and the droplet velocity field of a plain liquid jet injected into a high-pressure air crossflow. Additionally, the modeling results were compared with experimental data in terms of jet morphology. A coupled Σ -Y single-fluid Eulerian model was implemented in the OpenFOAM framework and was used for the CFD simulations. The new model includes a special treatment of the liquid diffusion due to drift-flux velocities and a new calibration of the spray atomization constants for jet in cross-flow, in comparison with previous works on diesel sprays. This study enables the further development of the drift-flux model on liquid jets injected in cross flow. Despite the drift-flux model proposed here, the experimental jet behavior is not fully retrieved, but the new model effect is noticeable, and the drift-flux consideration adds more physics to the classical model. There is still room to improve the current model, including also more validations against local properties, like velocities and droplet sizes, and exploring other turbulence models. The current work is a step in the direction towards a more predictive model of single fluid atomization.

6. References

- [1] Margason, R.J., 1993. Fifty years of jet in cross flow research. In AGARD.
- [2] Karagozian, A.R., 2010. Transverse jets and their control. *Progress in energy and combustion science*, 36(5), pp.531-553.
- [3] Karagozian, A.R., 2014. The jet in crossflow. *Physics of Fluids*, 26(10), pp.1-47.
- [4] Desclaux, A., Thuillet, S., Zuzio, D., Senoner, J.M., Sebbane, D., Bodoc, V. and Gajan, P., 2020. Experimental and numerical characterization of a liquid jet injected into air crossflow with acoustic forcing. *Flow, Turbulence and Combustion*, 105(4), pp.1087-1117.
- [5] Wu, P-K, Kirkendall, KA, Fuller, RP & Nejad, AS 1997, 'Breakup Processes of Liquid Jets in Subsonic Crossflows', *Journal of Propulsion and Power*, vol 31, pp. 309-319.
- [6] Sallam, KA, Aalburg, C & Faeth, GM 2013, 'Breakup of Round Nonturbulent Liquid Jets in Gaseous Crossflow', *AIAA Journal*, vol 13, pp. 64-73.
- [7] Broumand, M. and Birouk, M., 2016. Liquid jet in a subsonic gaseous crossflow: Recent progress and remaining challenges. *Progress in Energy and Combustion Science*, 57, pp.1-29.
- [8] Brown, C.T. and McDonnell, V.G., 2006, May. Near field behavior of a liquid jet in a crossflow. In *Proceedings of the ILASS Americas, 19th Annual Conference on Liquid Atomization and Spray Systems*.
- [9] Ishii, M. and Hibiki, T., 2010. *Thermo-fluid dynamics of two-phase flow*. Springer Science & Business Media.
- [10] Ishii, M. and Grolmes, M.A., 1975. Inception criteria for droplet entrainment in two-phase concurrent film flow. *AIChE Journal*, 21(2), pp.308-318.

- [11] Ishii, M., 1977. One-dimensional drift-flux model and constitutive equations for relative motion between phases in various two-phase flow regimes (No. ANL-77-47). Argonne National Lab., Ill.(USA).
- [12] Pandal, A., Ningegowda, B.M., Rahantamialisoa, F.N.Z., Zembi, J., Im, H.G. and Battistoni, M., 2021. Development of a drift-flux velocity closure for a coupled Σ -Y spray atomization model. *International Journal of Multiphase Flow*, 141, p.103691.
- [13] Elshamy, O. M., Tambe, S., Cai, J. and Jeng, S.M., 2006, January. Structure of liquid jets in subsonic crossflow at elevated ambient pressures. In 44th AIAA Aerospace Sciences Meeting and Exhibit (p. 1224).
- [14] Ishii, M., Jones, O. and Zuber, N., 1975. Thermal non equilibrium effects in the drift flux model of two-phase flow. *Transactions of the American Nuclear Society*, 22.
- [15] Elkotb, M.M., Mahdy, M.A. and Montaser, M.E., 1982. Investigation of external-mixing airblast atomizers. In *Proceedings of the 2nd international conference on liquid atomization and sprays* (pp. 107-115).
- [16] Rizkalla, A.A. and Lefebvre, A.H., 1975. The influence of air and liquid properties on airblast atomization. *Trans ASME J Fluids Eng* (97(3):316–20).
- [17] Lefebvre AH. Airblast atomization. *Prog Energy Combust Sci* 1980;6:233–61.
- [18] Elshamy, O. M., 2006. Experimental Investigations of Steady and Dynamic Behavior of Transverse Liquid Jets. Ph.D. thesis, University of Cincinnati.
- [19] Vallet A., Burluka A. A., and Borghi R., Development of a Eulerian Model for the “Atomization” of a Liquid Jet, *Atomization and Sprays*, vol. 11, pp. 619–642, 2001.
- [20] Rusche, H., Issa, R., 2000. The effects of voidage on the drag force on particles, droplets and bubbles in dispersed two-phase flow. In: *Proc. 2nd Japanese-European Two-Phase Flow Group Meeting*. Tsukuba (Japan).
- [21] Pandal, A., Rahantamialisoa, F., Ningegowda, B., and Battistoni, M., "An Enhanced Σ -Y Spray Atomization Model Accounting for Diffusion due to Drift-Flux Velocities," *SAE Int. J. Adv. & Curr. Prac. in Mobility* 2(5):2681-2690, 2020, <https://doi.org/10.4271/2020-01-0832>.